The FASEB Journal

FASEB
Federation of American Societies for Experimental Biology

RESEARCH ARTICLE OPEN ACCESS

PTPN2 Negatively Regulates Macrophage Immune Responses and Cellular Bioenergetics

Valerie Vinette[1,2] | Yevgen Zolotarov[1,2] | Alexandre Poirier[2,3] | Zuzet Martinez Cordova[1,2] | Isabelle Aubry[1,2] | Michel L. Tremblay[1,2,4]

[1]Department of Biochemistry, McGill University, Montreal, Canada | [2]Rosalind and Morris Goodman Cancer Institute, McGill University, Montreal, Canada | [3]Department of Experimental Medicine, McGill University, Montreal, Canada | [4]Department of Microbiology and Immunology, McGill University, Montreal, Canada

Correspondence: Michel L. Tremblay (michel.tremblay@mcgill.ca)

Received: 11 October 2024 | **Revised:** 18 March 2025 | **Accepted:** 1 April 2025

Funding: This work was supported by the Terry Fox oncometabolism grant TFF-116128, the Canadian Institute of Health Research Foundation grant (CIHR FDN-159923), the Richard and Edith Strauss Canada Foundation, and the Aclon Foundation.

Keywords: LysM-Cre | macrophages | proinflammation | protein tyrosine phosphatases | PTPN1 | PTPN2

ABSTRACT

PTPN2 is encoded by the protein tyrosine phosphatase N2 (also known as TC-PTP) and is a negative regulator of cytokine signaling and macrophage differentiation. In the past decade, our work and others, including several pharmaceuticals, have emphasized that inhibition of PTPN2 and PTPN1 (also known as PTP1B) may act as a new first-of-class cancer immunotherapeutic. Although the potential roles of these two enzymes in various immune cells have been broadly reported, the specific activity of PTPN2 in regulating macrophage immune and metabolic responses has yet to be fully elucidated. Hence, we sought to investigate the function of PTPN2 in macrophage polarization and on their activities. We used two different mouse models to systematically and specifically inhibit the expression of PTPN2 in macrophages and utilized a chemical inhibitor with a macrophage human cell line to assess their immune and metabolic profiles. We demonstrated that PTPN2 ablation in macrophages alters their immunometabolic transcriptome and enhances their proinflammatory response, as observed by increased IFN-ɣ and nitric oxide production. PTPN2 deficiency also leads to a dysregulation of mitochondrial respiration, as observed by decreased oxygen consumption and ATP production. We establish herein that PTPN2 dampens the proinflammatory response of macrophages while altering their mitochondrial respiration, validating its macrophage inhibition as a contributing factor in the potency of systemic dual inhibition of PTPN1 and PTPN2 against cancer.

1 | Introduction

Macrophages are the predominant type of phagocytic cells and, along with neutrophils, serve as the first line of defense in innate immunity [1, 2]. They secrete a plethora of cytokines and chemokines, including IFN-ɣ, IL-6, IL-10, IL-12, TNF-α, and CXCL10, which then activate other immune cells and attract them to the site of injury, leading to the initiation of an inflammatory cascade [3–7]. The protein tyrosine phosphatases (PTPs) PTPN1 and PTPN2 are known negative regulators of cytokine signaling. We have previously demonstrated that deletion of PTPN2 in mice is lethal at 3 weeks of age due to severe systemic inflammation caused in part by the upregulation of proinflammatory cytokines, including iNOS, TNF-α, and IFN-ɣ [8, 9]. We have further established that this PTP regulates macrophage development and activation by controlling the CSF-1R receptor [10, 11].

Over the past decade, it has been established that control of immune responses and metabolic homeostasis are closely

intertwined. We now understand that metabolic stresses can activate various pathways, such as NF-κB and HIF-1α, which can, in turn, upregulate inflammatory pathways and lead to inflammation [12, 13]. Similarly, inflammation can induce metabolic changes, as is the case in inflammatory bowel diseases when key glycolytic enzymes are upregulated [14]. In addition to its role as a negative regulator of inflammatory cytokine signaling, we have recently demonstrated that PTPN2 is a critical positive regulator of metabolism and mitochondrial respiration [15], proposing that this phosphatase may be necessary in the immunometabolic regulation of macrophages.

In addition to promoting inflammation and enabling the recruitment of immune cells, macrophages can also have anti-inflammatory functions, depending on the microenvironment and requirements. Although the plasticity of macrophages is now well accepted in the field [5, 6] and we now understand that macrophage polarization consists of a gradient of inflammatory phenotypes. For this study, we will consider homogeneous populations of proinflammatory macrophages (classically activated, termed M1) and anti-inflammatory macrophages (alternatively activated, referred to as M2). Various PTPs have been shown to regulate the polarization of macrophages, such as PTPN22, which is a positive regulator of M2 macrophage polarization [16]. In contrast, SHP-1 (PTPN6) and PTPN1 are negative regulators of M1 macrophage polarization upon induction by LPS [16]. Knowing the involvement of PTPs in reprogramming macrophages toward the proinflammatory M1 phenotype and the role of PTPN2 as a negative regulator of cytokine signaling, we were interested in studying the potential role of this phosphatase as a modulator of macrophage polarization and immunometabolic functions. This enthusiasm is compounded by the recent excitement to use dual inhibition of PTPN2 and its close relative PTPN1 in clinical oncology immunotherapeutics [17].

Herein, we focused our study on one of the putative anticancer activities of PTPN2 inhibition by demonstrating that PTPN2 is a negative regulator of proinflammatory macrophage polarization and immune responses. Additionally, loss of PTPN2 in macrophages leads to dysregulation of their transcriptome and aberrant induction of several pathways that promote immune responses, antigen processing and presentation, and mitochondrial respiration. We have also established that myeloid-specific deletion of PTPN2 leads to a similar phenotype in macrophages as a systemic deletion, albeit milder. Hence, deletion of PTPN2 solely in macrophages appears to be enough to induce inflammation. This effect is increased when the microenvironment, such as other immune cells and their corresponding cytokine production, is also deficient in PTPN2. The implication is that PTPN2 promotes macrophage immune responses in both a cell-intrinsic and cell-extrinsic manner. PTPN2 is crucial in macrophages to dampen inflammation and mitochondrial respiration that may result from inflammatory events such as tumor growth, infection, and injury.

2 | Material and Methods

2.1 | Mice

The generation of mice with a constitutive germline deletion of PTPN2 ($PTPN2^{-/-}$ mice, also known as $PTPN2^{-/-}$) has been described previously [8]. Heterozygous breeding pairs were used to ensure that wild-type, heterozygous, and knockout littermates were obtained for experiments. We also generated a myeloid-specific mouse model of PTPN2 deletion by breeding $PTPN2^{fl/fl}$ or $PTPN2^{fl/wt}$ C57BL/6 mice with LysM-Cre mice, as described previously by Spalinger et al. [18]. For experimental purposes, we crossed heterozygous (fl/wt) or knockout (fl/fl) PTPN2 mice, with one breeder being $Cre,^{+/-}$ to obtain $PTPN2^{fl/fl}$ LysM-$Cre^{+/-}$ knockout mice. All mice were housed in a specific pathogen-free facility in sterile microisolator caging. Animal protocols followed the regulations of the Canadian Council on Animal Care and were approved by the McGill University animal care committee.

2.2 | Isolation and Stimulation of Murine Immune Cells

Immune cells were harvested from two mouse models: the whole-body and myeloid-specific targeting of PTPN2. Bone marrow-derived macrophages (BMDMs) were generated by harvesting monocytes from the bone marrow, growing them in 10 cm^2 petri dishes in DMEM supplemented with 10% heat-inactivated fetal bovine serum, 1% GlutaMAX, 1% sodium pyruvate, 1% penicillin and streptomycin (Pen/Strep), 1% non-essential amino acids, and 0.1% β-mercaptoethanol, incubating them in a 5% CO_2 incubator at 37°C, and differentiating them into macrophages by stimulating them with 30 ng/mL recombinant murine M-CSF (PeproTech, 315–02) for 7 days. BMDMs were either maintained as naive macrophages (M0) or polarized toward the M1 proinflammatory phenotype using 20 ng/mL recombinant murine IFN-ɣ (PeproTech, 315–05) and 100 ng/mL lipopolysaccharide (LPS, Sigma-Aldrich, *E. coli* O55:B5) or toward the M2 anti-inflammatory phenotype using 20 ng/mL IL-4 (PeproTech, 214–14) for 24 h. For downstream experiments such as qRT-PCR, flow cytometry, and western blotting, macrophages plated in a 10 cm^2 Petri dish were harvested by washing twice with PBS, gently scraping with a cell scraper, and counting the cells.

2.3 | Cell Culture and Macrophage Differentiation

The human monocytic cell line U-937 (ATCC CRL-1593.2) was cultured in RPMI 1640 medium (Wisent Bioproducts) supplemented with 10% fetal bovine serum (FBS) (Hyclone, Fisher Scientific), 2 mM L-glutamine (Fisher Scientific), 10 mM HEPES (Wisent Bioproducts), 1 mM sodium pyruvate (Fisher Scientific), 4.5 g/L glucose, 1.5 g/L sodium bicarbonate (Hyclone, Fisher Scientific), 100 U/mL penicillin (Hyclone, Fisher Scientific), 100 μg/mL streptomycin (Hyclone, Fisher Scientific), and 0.05 mM β-mercaptoethanol (Fisher Scientific), and cultured in a 5% CO_2 incubator at 37°C. For macrophage differentiation, U-937 cells were cultured in six-well plates at a density of 400,000 cells/mL and treated with 100 ng/mL phorbol 12-myristate 13-acetate (PMA) (PeproTech) for 72 h. Media containing PMA was removed, and the cells were washed twice with PBS, followed by a recovery period of 24 h, during which new media was added. Differentiation into macrophages was confirmed by microscopic examination of cell morphology and evaluation of markers CD14, CD11b, CD11c,

and CD45RA expression by flow cytometry. Polarization of macrophages was carried out for 48 h by stimulation with 100 ng/mL LPS (*E. coli* 055:B5) and 25 ng/mL IFN-γ (PeproTech) to generate M1 macrophages and with 25 ng/mL IL-4 (PeproTech) to generate M2 macrophages. The absence of stimulation mimicked M0 macrophages. To inhibit PTPN2 and PTPN1, U-937 macrophage-like cells were treated for 30 min with 30 μM of the inhibitor L-598. Cells were washed twice with PBS and treated with polarization cytokines as described with 30 μM fresh L-598 for 48 h, after which cells were then processed for downstream analysis.

2.4 | RNA Isolation, Reverse Transcription and Quantitative Real-Time PCR

Total RNA was isolated from macrophages using TRIzol reagent (Thermo Fisher Scientific), according to the manufacturer's instructions. RNA was quantified with NanoDrop and the quality of the RNA was determined by running an RNA gel using with 500 ng RNA on a 1% agarose gel. Then, 1 μg of RNA was reverse transcribed to complementary DNA (cDNA) using the SuperScript III Reverse Transcriptase Kit (Thermo Fisher Scientific), as per the manufacturer's protocol. Quantitative real-time PCR (qRT-PCR) was performed with a LightCycler 480 (Roche) using SYBR Green Master Mix (Roche) according to the manufacturer's instructions. A panel of different housekeeping genes was tested with samples from different genotypes and polarization statuses, and *Actb* was determined to be the most reliable housekeeping gene for these conditions. It was, therefore, used as a reference gene to normalize the relative abundance of each gene of interest for all qRT-PCR experiments.

2.5 | Flow Cytometry

Fc receptors on purified BMDMs were blocked with an anti-CD16/CD32 antibody (BD Biosciences). Cell surface antigens were detected with the following antibodies diluted in PBS (Wisent) supplemented with 2.5% fetal bovine serum: phycoerythrin (PE)-conjugated anti-F4/80, fluorescein isothiocyanate (FITC)-conjugated anti-CD11b, PE/Dazzle 594 anti-CD80, pacific blue (PB) anti-CD86, and peridinin–chlorophyll protein (PerCP)-Cy5.5-conjugated anti-CD301 from BioLegend. For experiments requiring the detection of intracellular antigens or cytokines by flow cytometry, cells were fixed and permeabilized after the extracellular staining and then stained for the following intracellular markers: allophycocyanin (APC)-conjugated anti-NOS2 (Thermo Fisher Scientific) and PE-Cy7-conjugated anti-IFN-ɣ or PE-Cy7-conjugated anti-CD206 (BioLegend). F4/80 and CD11b were used as general macrophage markers, NOS2, CD80, and CD86 as M1 macrophage markers, and CD206 and CD301 as M2 macrophage markers. All cells were stained with the Live/Dead fixable Aqua viability dye (Thermo Fisher Scientific). For the U-937 cell line, FITC-conjugated anti-CD14 (clone M5E2, BD), APC-conjugated anti-CD11b (clone ICRF44, BD), PE-conjugated anti-CD11c (clone 3.9, BD), and PerCP-Cy5.5-conjugated anti-CD45RA (clone HI100, BD) were used.

For CXCL9 and CXCL10, intracellular staining was performed using BD GolgiPlug for 4 h. Cells were washed twice with PBS, gently detached, and resuspended in FACS buffer (2% FBS in PBS). To block nonspecific binding, the cells were incubated with Human TruStain FcX (BioLegend) for 10 min at 4°C. Cells were then stained with a viability dye (LIVE/DEAD Fixable Aqua Dead Cell Stain Kit, Invitrogen) for 30 min at 4°C. Intracellular staining was performed using the Cytofix/Cytoperm kit (BD) as per the manufacturer's directions. The detection of CXCL9 and CXCL10 was performed using APC-conjugated anti-CXCL9 (clone J1015E10, BioLegend) and PE-conjugated anti-CXCL10 (clone J034D6, BioLegend). Samples were acquired using a FACSCanto II or LSRFortessa (BD Biosciences) and analyzed with FlowJo software (Tree Star).

2.6 | RNA-Sequencing and Data Analysis

RNA from purified BMDMs was isolated with TRIzol and purified with the PureLink DNase Set (Thermo Fisher Scientific), according to the manufacturer's protocol. Samples were subjected to RNA-sequencing (RNA-Seq) using an Illumina HiSeq 2500. Transcript abundances were quantified with Kallisto v0.41.1 [19] using paired-end reads pseudo-aligned to the mouse transcriptome (GENCODE M17). Differential gene expression analysis was performed by importing Kallisto results with tximport v1.6.0 [20], followed by DESeq2 v1.18.1 [21]. Genes were filtered based on adjusted *p* value below 0.05 and log-transformed expression fold change of 2 or more. InnateDB and gene ontology (GO) were used for downstream analysis to identify pathways and biological processes enriched in specific populations.

2.7 | Enzyme-Linked Immunosorbent Assays and Nitric Oxide Production Assay

BMDMs were harvested and generated from $PTPN2^{+/+}$ (systemic wild-type, WT), $PTPN2^{+/-}$ (systemic heterozygous, HET), and $PTPN2^{-/-}$ (systemic knockout, KO), or from $PTPN2^{fl/fl}$ LysM-$Cre^{-/-}$ (WT) and $PTPN2^{fl/fl}$ LysM-$Cre^{+/-}$ (myeloid-specific KO) mice. Cells were divided into three populations and plated in 10 cm^2 Petri dishes: an unstimulated population of naive BMDMs (M0), proinflammatory macrophages (M1) and anti-inflammatory macrophages (M2). After cells were polarized for 24 h, 2 mL of supernatant from each dish was collected, transferred to a microcentrifuge tube, centrifuged at 10000 rpm at 4°C to remove cell debris, and the supernatant was transferred to a clean microcentrifuge tube for analysis. Enzyme-linked immunosorbent assays (ELISAs) were performed according to the manufacturer's protocol to quantify the cytokines IFN-ɣ, IL-6, and CXCL10 expression. To assess the nitric oxide (NO) production of M0, M1, and M2 macrophages, the Griess Reagent System (Promega, G2930) was used according to the manufacturer's protocol. Data were normalized to cell number for all ELISAs and NO production experiments by performing a CyQUANT assay (Thermo Fisher Scientific, C7026), according to the manufacturer's protocol.

2.8 | Western Blotting

Total cell lysates (TCL) were prepared using modified radioimmunoprecipitation assay (mRIPA) buffer (50 mM Tris–HCl (pH 7.5), 150 mM NaCl, 0.25% sodium deoxycholate and 1% NP-40) supplemented with EDTA-free protease inhibitor (Roche) and 2 mM sodium orthovanadate (Sigma-Aldrich). Protein levels were quantified by bicinchoninic acid (BCA) assay. 15 μg of each lysate was run on 10% SDS-PAGE gels using the antimouse primary antibody PTPN2 (1/10, homemade clone 3E2), as well as the antirabbit primary antibodies STAT3 (Cell Signaling Technology), p-STAT3 (Tyr705, Cell Signaling Technology), STAT1 (Cell Signaling Technology), and p-STAT1 (Tyr701, Cell Signaling Technology). The antirabbit primary antibody β-actin was from Cell Signaling Technology, and secondary antibodies antimouse and antirabbit HRP were obtained from Jackson ImmunoResearch. Each lane represents an individual mouse. Blots were imaged using the Mini-Medical Series imager (AFP Imaging).

2.9 | Seahorse XF Assays

Metabolic changes in oxygen consumption rate (OCR) were measured using a Seahorse XFe96 extracellular flux (XF) analyzer (Agilent). Cells were harvested from the bone marrow of PTPN2 WT, HET, or KO mice or $PTPN2^{fl/fl}$ LysM-$Cre^{-/-}$ (WT) and $PTPN2^{fl/fl}$ LysM-$Cre^{+/-}$ (KO) mice and seeded in 10 cm^2 Petri dishes. Cells were allowed to differentiate for 7 days with 30 ng/mL M-CSF and cultured in a 5% CO_2 incubator at 37°C. Fresh M-CSF was supplemented every 3 days. Prior to performing the Seahorse XF assay, cells were detached by scraping and seeded at 45000 cells/well in an XFe96 microplate in 80 μL media supplemented with 30 ng/mL M-CSF. Cells were allowed to attach for 1 h at room temperature and then for 2 h in the incubator prior to the addition of polarization media. BMDMs were polarized to pro- or anti-inflammatory macrophages by adding 20 μL of media supplemented with LPS (M1) or IL-4 (M2) for 24 h. 20 μL fresh media was added to a subset of cells to maintain naive (M0) BMDMs.

On the day of the assay, 50 μL of the media was gently removed from the wells using a multichannel pipette, cells were washed twice with XF assay medium (Agilent, 102 353–100), and fresh XF assay medium was added. The plate was incubated for 1 h in a CO_2-free incubator at 37°C to equilibrate. The cell plate was then transferred to the XFe96 extracellular flux analyzer. The assay was performed with four cycles for the basal state and four after each injection, where each cycle consisted of a 3-min mix and a 3-min measure period. To measure mitochondrial respiration, oligomycin (Sigma-Aldrich, #O4876), FCCP (carbonyl cyanide-4-[trifluoromethoxy]phenylhydrazone, Sigma-Aldrich, #C2920), rotenone (Sigma-Aldrich, #R8875), and antimycin A (Sigma-Aldrich, #A8674) were added at a final concentration of 1.5 μM, 2 μM, 1.5 μM, and 2 μM, respectively, at specific time points to inhibit different complexes of the electron transport chain. To measure the extracellular acidification rate, 25 mM glucose, 1.5 μM oligomycin, and 50 mM 2-deoxy-D-glucose (2-DG) were used. Each assay was performed with at least five replicates and normalized to cell number by performing a CyQUANT assay per the manufacturer's protocol.

2.10 | Statistical Analyses

Many of the experiments were analyzed using one-way analysis of variance (ANOVA) with Tukey's multiple comparisons test. Other experiments were analyzed with a *t*-test, and those with two independent variables were analyzed using a two-way analysis of variance (2way ANOVA) with a Šídák post hoc multiple correction, as specified in the figure legends.

3 | Results

3.1 | PTPN2 Deficiency Favors the Reprogramming of Macrophages to Proinflammatory M1 Macrophages

To study the effect of PTPN2 on macrophage polarization and function, we first established a panel of genes characteristic of pro- (M1) or anti- (M2) inflammatory macrophages, with little to no expression in other macrophage subsets. To do this, we curated the literature and identified a group of 11 genes that were most often used to characterize M1 or M2 BMDMs: *Ccr7*, *Cxcl11*, *Il12b*, *Nos2*, *Ptgs2*, and *Tnf* for M1 macrophages, and *Arg1*, *Ccl24*, *Chil3*, *Retnla*, and *Ptgs1* for M2 macrophages [22–28]. We assessed these by qRT-PCR using naive BMDMs (M0) derived from wild-type mice and polarized toward M1 or M2 macrophages (list of all genes used in Figure S1). This allowed us to identify *Ccr7*, *Cxcl11*, *Il12b*, *Nos2*, *Ptgs2*, and *Tnf* as being robust M1 macrophage-specific genes, while *Arg1* and *Retnla* are robust M2 macrophage-specific genes (Figure S2). As such, we used *Cxcl11* and *Tnf* genes as representative M1 genes and *Arg1* and *Retnla* as representative M2 genes when assessing macrophage polarization in subsequent experiments.

With these polarization genes clearly defined, we next sought to identify the inflammatory phenotype of BMDMs harvested from PTPN2 wild-type (WT), heterozygous (HET) or knockout (KO) mice. Compared with their WT and HET counterparts, we observed a considerable upregulation of M1 genes *Cxcl11* and *Tnf* in PTPN2 KO macrophages (Figure 1A), indicating an enhanced transcriptional modulation of proinflammatory genes in macrophages lacking PTPN2. While the M2 gene *Retnla* was unchanged across genotypes in M2 macrophages, *Arg1* was upregulated in a dose-dependent manner, with the highest expression observed in M2 KO macrophages (Figure 1B). This could be due to upstream signaling via STAT6, which is a known regulator of M2 macrophage polarization and has been demonstrated to bind directly to the promoter region of *Arg1*, leading to induction of its gene expression [29, 30]. STAT6 is a known substrate of PTPN2 [31]. Hence, the absence of this tyrosine phosphatase would result in increased STAT6 phosphorylation and activation, leading to subsequent upregulation of *Arg1*.

Next, we performed flow cytometry with these BMDMs using the M1 marker NOS2 and the M2 markers CD206 (aka MRC1) and CD301 to determine whether these transcriptional changes are reflected at the protein level. We established that there is an upregulation of the M1 marker NOS2 in PTPN2-deficient M1 BMDMs compared to WT and HET counterparts (Figure 1C), both in the number of cells that express this marker (Figure 1D) and in the amount of NOS2 expressed (geometric mean

fluorescent intensity, gMFI, Figure 1E). On the other hand, the expression of the M2 markers CD206 (Figure 1F,G) and CD301 (Figure 1H,I) was independent of PTPN2 levels. Except for *Arg1*, a STAT6 target gene, we found no evidence for increased polarization of alternatively activated (M2) macrophages. These data suggest that the ablation of PTPN2 in mice gives rise to macrophages that are more apt at polarizing toward a proinflammatory phenotype.

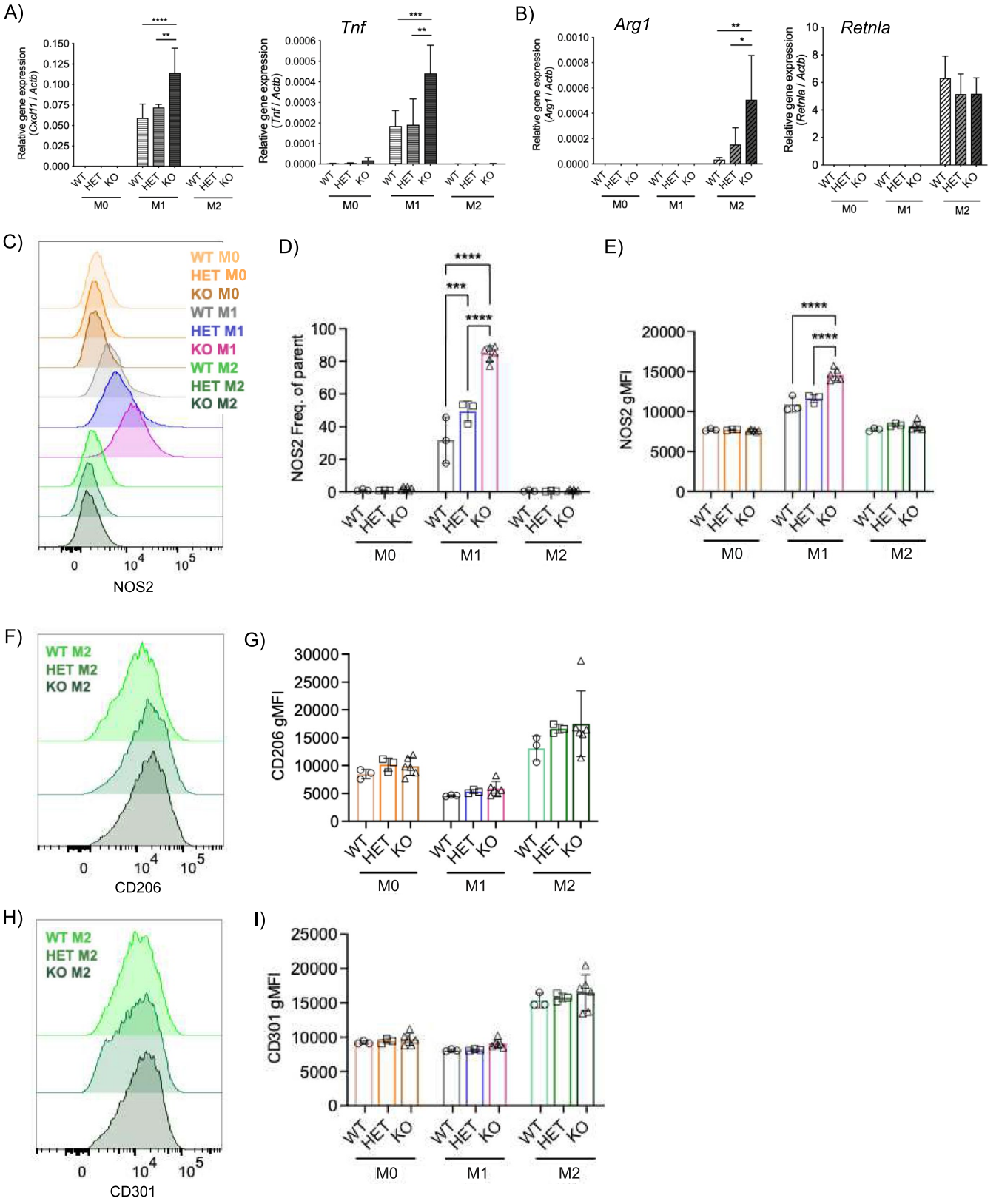

FIGURE 1 | Legend on next page.

FIGURE 1 | Macrophage polarization toward the M1 proinflammatory state is favored upon deletion of PTPN2. (A and B) Measurement of gene expression by qRT-PCR for genes characteristic of proinflammatory (A) and anti-inflammatory (B) BMDMs in naive (M0), M1-, and M2-polarized macrophages harvested from PTPN2 wild-type (WT), heterozygous (HET) and knockout (KO) mice. Data represent the mean ± SD of two to five biological replicates performed in three independent experiments. (C–I) Flow cytometry analysis of M0, M1, and M2 BMDMs derived from PTPN2 WT ($n = 3$), HET ($n = 3$) and KO ($n = 5$) mice. Data represent the mean ± SD of one experiment from three independent experiments. (C) Histogram representation of expression of M1-marker NOS2 with corresponding frequency of parent (D) and geometric mean fluorescence intensity (gMFI, E) analyses. (F) Histogram representation of expression of M2-marker CD206 in M2 BMDMs with corresponding gMFI analysis (G). (H) Histogram representation of expression of M2-marker CD301 in M2 BMDMs with corresponding gMFI analysis (I). *$p < 0.05$, **$p < 0.01$, ***$p < 0.005$, ****$p < 0.001$ based on two-way ANOVA with Tukey's multiple comparisons test.

3.2 | PTPN2 Governs the Proinflammatory Phenotype of Macrophages

To further investigate the role of PTPN2 in regulating the immunophenotype of macrophages, we performed bulk RNA-sequencing with macrophages harvested from PTPN2 WT, HET, and KO mice maintained in a naïve state (M0) or stimulated to proinflammatory (M1) or anti-inflammatory (M2) macrophages. InnateDB pathways analysis and gene ontology (GO) enrichment analysis were performed to identify pathways and biological processes modulated in PTPN2-deficient macrophages in different polarization states. We discovered that the pathways of "*innate immune response*" and "*positive regulation of cell migration*," were underrepresented in PTPN2 knockout proinflammatory BMDMs compared to wild-type and heterozygous cells (Figure 2A,B). On the other hand, several pathways, such as "*antigen processing*" and "presentation of exogenous peptide antigen via MHC class II," were instead overrepresented in these macrophages (Figure 2C). This was characterized by a much higher number of modulated genes in proinflammatory macrophages than in unstimulated cells (M0) or anti-inflammatory macrophages (Figure 2D).

We generated Venn diagrams to tease apart transcriptional reprogramming in these macrophages based on differentially expressed genes (DEGs) to identify genes exclusively or commonly modulated between M0, M1, and M2 macrophages (Figure 2E,F). We found that the vast majority of DEGs upregulated in KO BMDMs were in the proinflammatory M1 subset (Figure 2E), such as the macrophage chemoattractants *Cxcl9* and *Cxcl11* [32, 33] and *Clec9a*, which is involved in cross-presentation and activation of cytotoxic $CD8^+$ T cells [34, 35]. Clec9 also enables macrophages to clear dead cells to prevent chronic inflammation [36]. *Ido1* is another gene exclusively upregulated in KO M1 macrophages (Figure 2E). Notably, *Ido1* is a crucial factor in maintaining a balance between immune activation and suppression, ensuring a control of excessive inflammation that is often observed during responses to intracellular pathogens, cancer, or autoimmune diseases [37, 38].

Interestingly, a small subset of genes was upregulated in KO BMDMs compared to WT in all M0, M1, or M2 macrophages. This includes *Icam2*, which is involved in cell adhesion and is crucial for the migration of macrophages to sites of inflammation, which is essential upon induction of systemic inflammation in mice resulting from the deletion of PTPN2. On the other hand, hundreds of DEGs were downregulated in KO macrophages of different polarization states, with M1 KO macrophages experiencing the most drastic transcriptional reprogramming, with almost 400 genes being exclusively downregulated in this group (Figure 2F). This subset of genes includes *Tlr7* and *Tlr8*, two toll-like receptors (TLRs) that are necessary for the recognition of pathogen-associated molecular patterns (PAMPs) and initiating immune responses [39, 40]. These TLRs are also involved in the production of TNF-α and IL-6 through the recruitment of MyD88 and activation of downstream signaling cascades that ultimately lead to the activation of transcription factor NF-κB [41–43]. *Ccl2* (also known as MCP-1) and *Ccl5* (also known as RANTES) are also downregulated exclusively in KO M1 macrophages (Figure 2F). These chemokines are involved in the recruitment of macrophages at the site of inflammation or injury [44, 45]. Since the induction of either chemokine can lead to excessive recruitment of macrophages and contribute to chronic inflammation, the downregulation of these chemokines would be essential in dampening chronic inflammation that results from systemic PTPN2 depletion to avoid tissue damage.

We used InnateDB and GO to identify pathways modulated in PTPN2-deficient macrophages. "*Cell signaling*", "*cell proliferation*" and "*cell adhesion*" seem more affected in naive macrophages, while cytokine signaling was more prominent in M2 macrophages. On the other hand, many more pathways were significantly underrepresented in proinflammatory knockout macrophages, several involving chemotaxis of various immune cells, cytokine signaling, and response to stimuli such as interferons or viruses (Figure 2G). Several immune pathways were enriched in PTPN2-deficient proinflammatory macrophages, such as "*PD-1 signaling*," "*response to IFN-γ*," "*antigen processing and presentation*," and "*TCR signaling*." Interestingly, many metabolic pathways were also overrepresented in these M1 macrophages, including "*respiratory electron transport*" and "*oxidative phosphorylation*" (Figure 2H). Other pathways relating to "*cell cycle*," "*DNA repair*," and "*DNA replication*" were enriched in M0 and M2 macrophages but not in M1 in absence of PTPN2 (Figure 2H). These results indicate that PTPN2 deficiency leads to a stark transcriptional reprogramming in macrophages, characterized by upregulation of several immune and metabolic pathways. This hyperactivation is even more pronounced in proinflammatory macrophages.

Following our discovery that many immune pathways were dysregulated in PTPN2-deficient proinflammatory macrophages, we performed qRT-PCR analysis with M1-polarized BMDMs to validate some hits. We confirmed that a subset of immune genes, notably *Ccl2*, *Ccl3*, and *Marco*, were downregulated in knockout cells (Figure S3A). Ccl2 and Ccl3 are potent proinflammatory chemokines for macrophages and other immune cells [46–48]. Marco is a scavenger receptor

molecule that mediates nonopsonin-dependent phagocytosis, which is essential in macrophages for activating an immune response necessary to clear foreign pathogens [49, 50] and has also been demonstrated to be highly expressed on tumor-associated macrophages (TAMs) [51]. On the other hand, the expression of *Ccr2*, a receptor for Ccl2 that is highly expressed

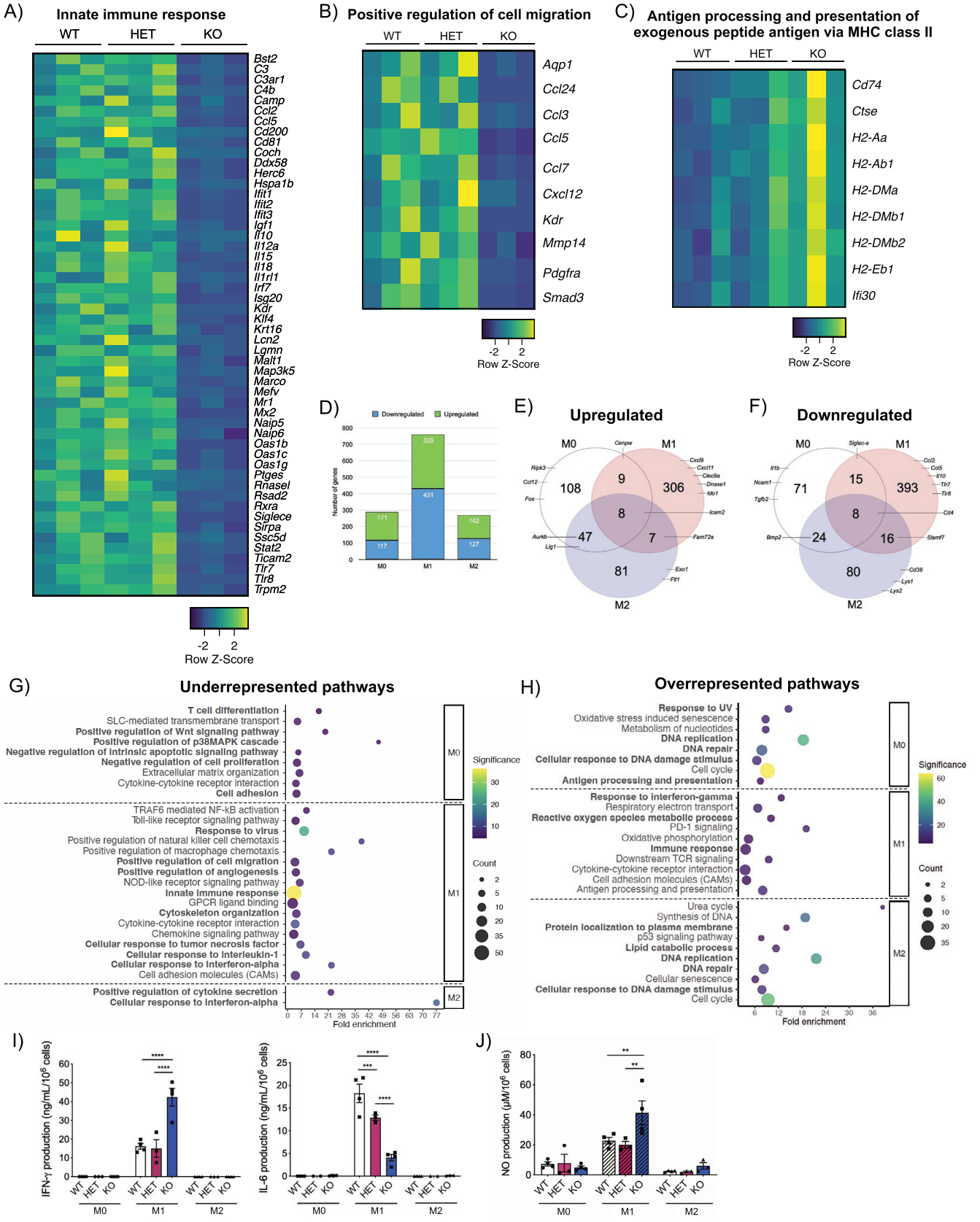

FIGURE 2 | Legend on next page.

FIGURE 2 | PTPN2 deletion enhances the proinflammatory phenotype of macrophages. RNA-Seq was performed with M0-, M1-, and M2-polarized BMDMs harvested from PTPN2 wild-type (WT), heterozygous (HET), and knockout (KO) mice. (A–C) Heatmaps generated based on differentially expressed genes in WT, HET, and KO M1 BMDMs. Genes involved in innate immune response (A), cell migration (B), and antigen processing and presentation of exogenous peptide antigen via MHC Class II (C). (D–F) Venn diagrams representing shared genes or those exclusively present in M0, M1, and M2 BMDMs. (D) Number of genes downregulated and upregulated in KO BMDMs depending on the macrophage polarization status. Number of genes that are upregulated (E) or downregulated (F) in KO vs. WT BMDMs. (G, H) Gene ontology (GO) enrichment analysis was performed to identify pathways and biological processes enriched in WT and KO M0, M1 and M2 macrophages. Data represent three mice per genotype and -log (corrected *p* value) of 1.3 was set as a threshold to assess underrepresented (F) or overrepresented (G) pathways in KO BMDMs. (I) IFN-ɣ and IL-6 cytokine production by M0, M1, and M2 BMDMs was assessed by ELISA. Data represent 3 to four mice per condition. (J) NO production from WT, HET, and KO BMDMs was determined. Data represent 3 to four mice per condition. $^{**}p < 0.01$, $^{***}p < 0.005$, $^{****}p < 0.001$ based on two-way ANOVA with Tukey's multiple comparisons test.

on proinflammatory macrophages [52], was upregulated. We also observed a substantial upregulation of proinflammatory genes *Cxcl10*, *H2-Aa*, *H2-Ab1*, and *Il12rb2* in PTPN2-deficient macrophages (Figure S3B).

We further assessed the consequence of PTPN2 deficiency by measuring cytokine production. We established that M1 KO macrophages secrete more than double the IFN-ɣ as WT or HET macrophages. IL-6 production was conversely decreased considerably in a PTPN2 dose-dependent manner (Figure 2I), which could be explained by the downregulation of *Tlr7* and *Tlr8* in KO M1 macrophages. Finally, as expected, we demonstrated that PTPN2 ablation enhances nitric oxide production solely by M1 macrophages since levels were barely detectable in M0 or M2 macrophages (Figure 2J). These data together support the premise that PTPN2 deficiency enhances the proinflammatory immune responses of macrophages.

3.3 | Generation and Validation of PTPN2/LysM-Cre Mouse Model

In our systemic mouse model with a germline deletion of PTPN2, we have shown that macrophages generated are more apt at polarizing toward M1 macrophages with an enhanced proinflammatory signature. While the transcriptome of naive and anti-inflammatory BMDMs was somewhat affected by the inhibition of PTPN2, that of proinflammatory macrophages was considerably dysregulated. PTPN2-deficient M1 macrophages displayed an upregulation of pathways involved in regulating the immune response and its activation, as well as in several metabolic pathways. These data left us wondering whether a constitutive deletion of this phosphatase is required for the observed phenotype in macrophages or whether PTPN2 could also have a cell-intrinsic effect. To answer this question, we generated a LysM-Cre mouse model where deletion of PTPN2 would be restricted to myeloid cells and, more specifically, macrophages. Although other cells from the myeloid compartment may be affected, such as neutrophils and dendritic cells, macrophages are typically the primary myeloid cell type affected by the Cre recombinase inserted into the lysozyme 2 gene [18, 53–55]. Upon generation of PTPN2/LysM-Cre mice, we validated the efficient knockdown of PTPN2 exclusively in myeloid cells.

We performed western blotting to determine the expression of PTPN2 in these various immune cell types. Since the LysM-Cre mouse model only targets cells from the myeloid compartment, PTPN2 should only be deleted in macrophages. Indeed, inhibition of PTPN2 was observed only in macrophages and dendritic cells (Figure S4A). Additionally, deletion of PTPN2 seemed to be more efficient in macrophages compared to dendritic cells, which has been previously reported in different LysM-Cre mouse models [18, 53, 55]. We observed normal, unchanged expression of PTPN2 in B and T cells (Figure S4B), regardless of the genotype of the mice. These data confirm that PTPN2 deletion in our PTPN2/LysM-Cre mice is only observed in myeloid cells and more so in macrophages.

3.4 | Macrophage-Specific Deletion of PTPN2 Leads to an Enhanced Proinflammatory Phenotype

To validate the macrophage phenotype observed in the systemic mouse model of PTPN2 deletion, we assessed the expression of polarization genes in M0, M1, and M2 macrophages derived from PTPN2 LysM-Cre by qRT-PCR. Compared to their WT counterparts, proinflammatory genes *Cxcl11* and *Ccr7* were upregulated in $PTPN2^{fl/fl}$ LysM-$Cre^{+/-}$ knockout BMDMs (Figure 3A). On the other hand, anti-inflammatory genes *Arg1* and *Retnla* were not modulated in M2 macrophages (Figure 3B), indicating a preferential upregulation of the proinflammatory signature. We next performed western blotting for proteins that we previously established to be regulated by PTPN2, notably STAT1 and STAT3, and we observed very little phosphorylated STAT1 or STAT3 in naive macrophages, independent of the presence of PTPN2. However, we observed a distinct increase in the phosphorylation of both STAT1 and STAT3 in KO M1 macrophages compared to WT (Figure 3C), suggesting enhanced activation of these transcription factors in the absence of PTPN2. Flow cytometry analysis allowed us to identify an increased expression of the M1 markers CD80 and CD86 in PTPN2 KO M1 BMDMs (Figure 3D). At the same time, we did not observe any difference in the expression of the M2 marker CD206 (Figure 3E), validating the results obtained with our systemic PTPN2-deficient mouse model. Interestingly, in this LysM-Cre model, we observed a slight decrease in NOS2 expression in PTPN2-deficient proinflammatory BMDMs, which we did not observe with our first model (Figure 1C–E), perhaps pointing to a PTPN2-dependent cell-intrinsic role in the regulation of NOS2.

Considering the observed upregulation of STAT1 and STAT3 phosphorylation in proinflammatory macrophages, we sought

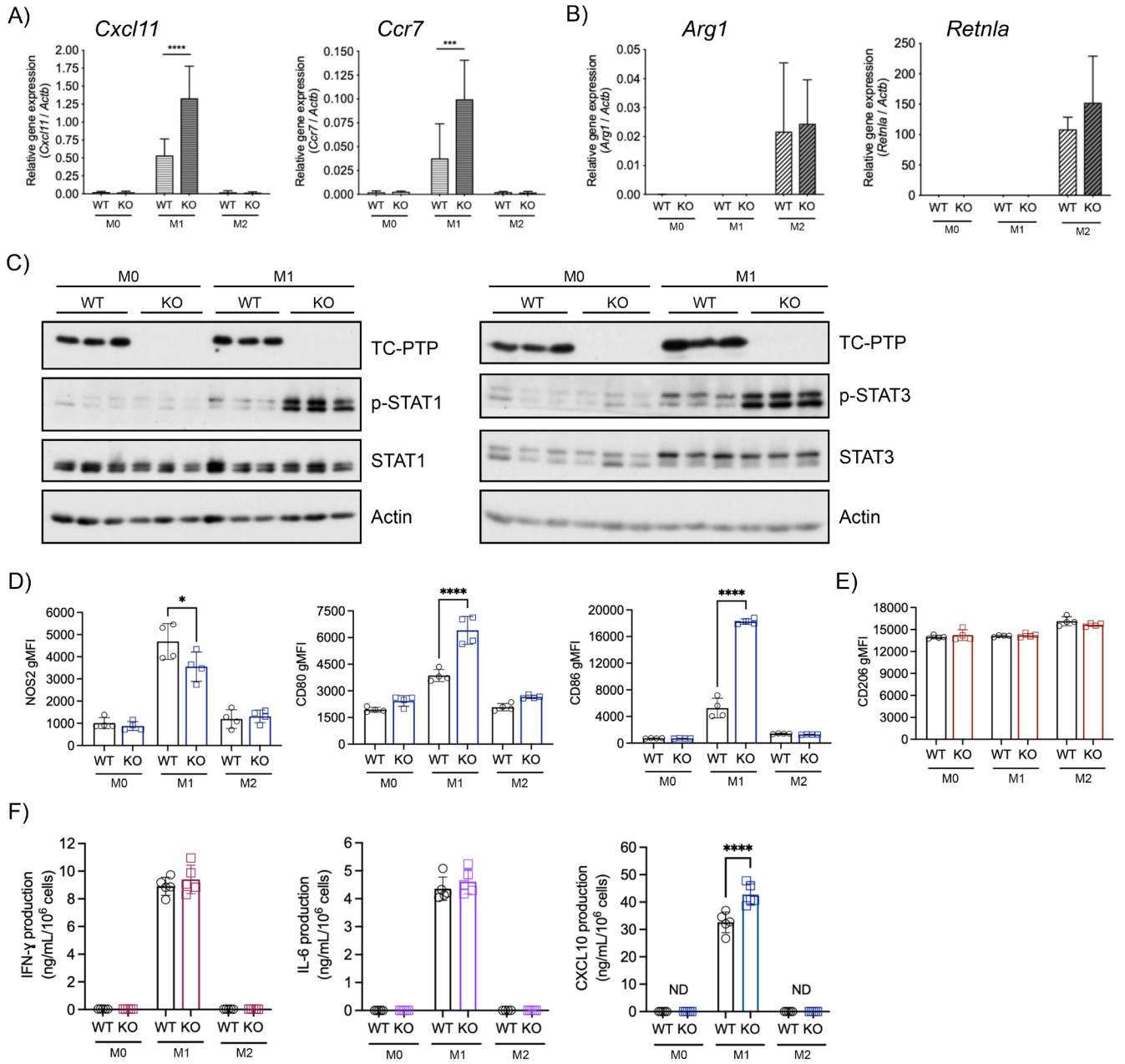

FIGURE 3 | Enhanced proinflammatory immune response in PTPN2$^{fl/fl}$ LysM-Cre BMDMs. BMDMs harvested from WT and PTPN2$^{fl/fl}$ LysM-Cre (KO) mice were maintained in a naive state (M0) or stimulated with IFN-ɣ and LPS (M1) or IL-4 (M2) for 24 h. qRT-PCR measurements of genes characteristic of M1 (A) and M2 (B) macrophages to assess gene expression. Data represent the mean ± SEM of five biological replicates. (C) Western blot analysis of PTPN2, pSTAT1, STAT1, pSTAT3, STAT3, and Actin. (D) Flow cytometry analysis of markers characteristic of M1 macrophages (NOS2, CD80, and CD86). (E) Flow cytometry analysis of marker characteristic of M2 macrophages (CD206). (F) IFN-ɣ, IL-6, and CXCL10 cytokine production was assessed from M0, M1, and M2 WT and PTPN2$^{fl/fl}$ LysM-Cre KO BMDMs. Data represent the mean ± SEM of three to five biological replicates. *$p < 0.05$, ***$p < 0.005$ and ****$p < 0.001$ based on two-way ANOVA with Šídák's multiple comparison test.

to determine whether downstream cytokine signaling would be altered in these macrophages. While the production of IFN-ɣ and IL-6 was independent of PTPN2 expression in this model, we observed an upregulation of CXCL10 upon inhibition of PTPN2 in M1 macrophages (Figure 3F), indicating that immune cell recruitment might be more critical in this model, possibly via a CXCL10-STAT1 signaling axis. These data suggest that PTPN2 ablation leads to an enhanced proinflammatory phenotype in macrophages derived from LysM-Cre mice.

3.5 | Inhibition of PTPN2 in Human Macrophages Enhances the Proinflammatory Immune Response

Having observed the effect of genetic PTPN2 ablation on the immune phenotype of macrophages and knowing the great potential of PTPN1/PTPN2 inhibitors in immunotherapy, we used a chemical inhibitor of PTPN2 and PTPN1 (PTPN2/PTPN1, aka N2/N1) L-598 to assess the effect in a human macrophage-like cell line U-937. At the transcriptomic level,

we observed a sturdy upregulation in the macrophage and immune cell chemoattractants *CXCL9*, *CXCL10*, and *CXCL11* in M1-polarized U-937 cells upon chemical inhibition of N2/N1 (Figure 4A). Next, we investigated the expression of downstream targets of N2/N1 by western blotting and observed an upregulation of phosphorylated STAT1 and STAT3 in M1 U-937 cells treated with the L-598 inhibitor (Figure 4B). Flow cytometry analysis showed us that a higher percentage of M1-polarized U-937 cells expressed CD14 upon inhibition of N2/N1 (Figure 4C). Similarly, significantly more human M1 macrophage-like cells expressed CD38 (Figure 4D), CXCL9 (Figure 4E), and CXCL10 (Figure 4F) upon inhibition of N2/N1, as well as expressing a higher amount of these proinflammatory markers and chemoattractants in the absence of these PTPs. These data indicate that this N2/N1 L-598 inhibitor is effective at dampening the activity of PTPN2/N1 in macrophages, as observed by upregulation of their downstream targets and proinflammatory markers CD14, CD38, CXCL9, CXCL10, and CXCL11.

3.6 | Mitochondrial Respiration Is Dysregulated in the Absence of PTPN2 in Proinflammatory Macrophages

In addition to the modulation of several pathways related to immune responses, we found particularly intriguing that inhibition of PTPN2 in proinflammatory macrophages also led to the overrepresentation of several metabolic pathways, including *respiratory electron transport* (Figure 5A). Most of the genes represented in this pathway are part of different complexes of the ETC, as portrayed in the schematic diagram (Figure 5B). We performed qRT-PCR to validate the expression of various metabolic genes. We observed a considerable upregulation in KO M1 macrophages compared to WT and HET cells, including *Atp5mc1*, *Cox7b*, *Ido1*, *Ido2*, and *Tomm40* (Figure S3C). Atp5mc1 and Cox7b are part of complex V (ATP synthase) and IV (cytochrome c oxidase) of the electron transport chain (ETC), respectively. At the same time, Tomm40 is required to move proteins into the mitochondria. Ido1 and Ido2, on the other hand, are

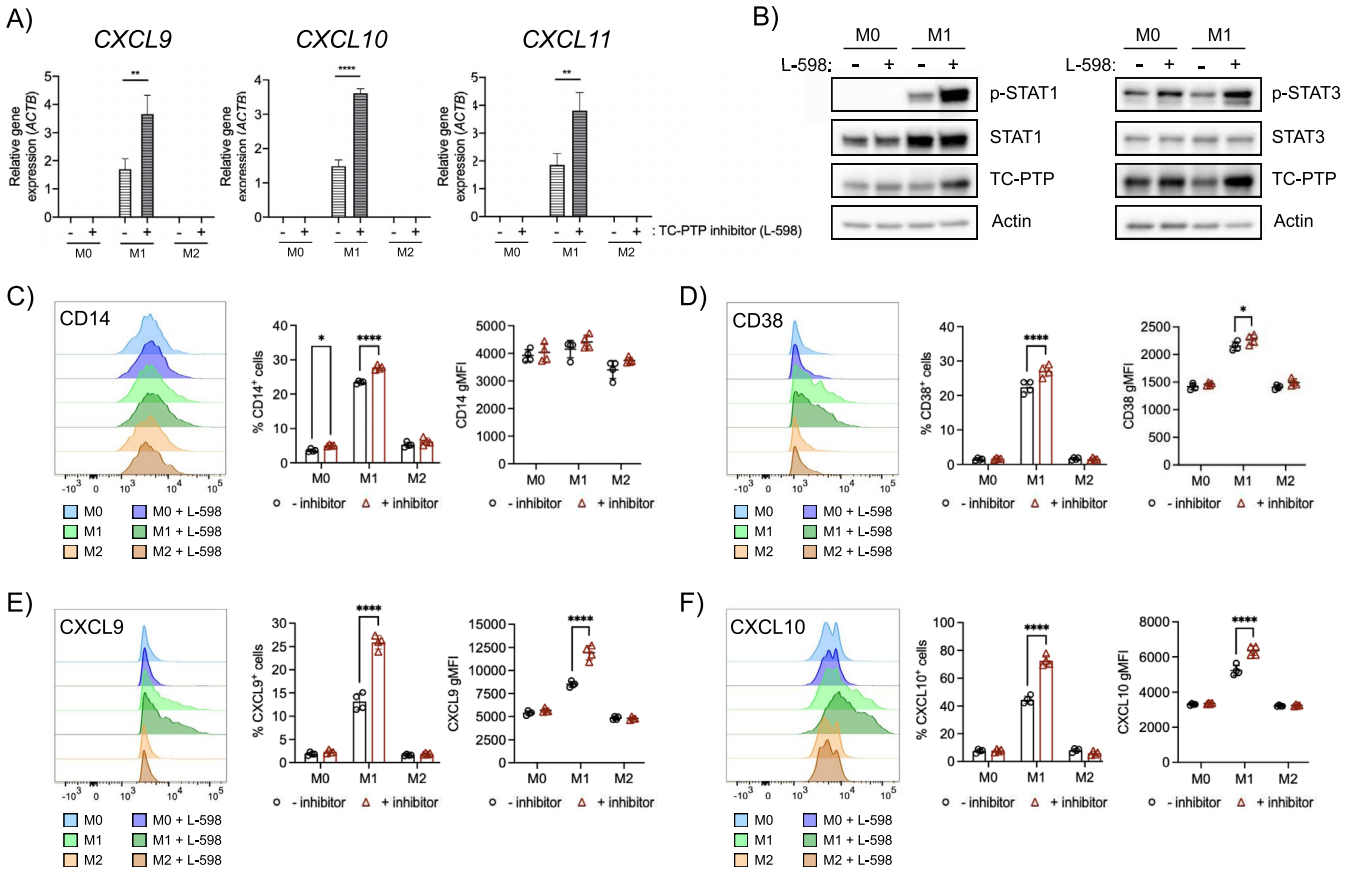

FIGURE 4 | Inhibiting PTPN2 in human macrophages promotes a proinflammatory immune response. Human macrophage-like U-937 cell line was used and treated with 30 μM PTPN2/PTPN1 inhibitor L-598 for 30 min. Cells were kept unstimulated (M0) or polarized toward the M1 phenotype with 100 ng/mL LPS and 25 ng/mL IFN-γ, or toward the M2 phenotype with 25 ng/mL IL-4. Cells were harvested for downstream experiments. (A) Measurement of gene expression by qRT-PCR for proinflammatory chemoattractant genes *CXCL9*, *CXCL10* and *CXCL11* in M0, M1, and M2 U-937 macrophages with or without inhibition of N2/N1. Data represent one of three independent experiments performed with four technical replicates. $^{**}p < 0.01$, $^{****}p < 0.001$ based on two-way ANOVA with Šídák multiple comparisons test. (B) Western blot performed with M0 and M1 U-937 cells treated with L-598 to assess expression of phosphorylated STAT1, STAT1, phosphorylated STAT6, STAT6, TC-PTP, and Actin. (C–F) Flow cytometry analysis of M0, M1, and M2 U-937 cells treated or not with N2/N1 inhibitor L-598. Data represent one of three independent experiments performed with four technical replicates. $^{*}p < 0.05$, $^{****}p < 0.001$ based on two-way ANOVA with Šídák multiple comparisons test. Histogram representation, frequency of cells, and geometric mean fluorescence intensity (gMFI) of markers CD14 (C), CD38 (D), CXCL9 (E), and CXCL10 (F).

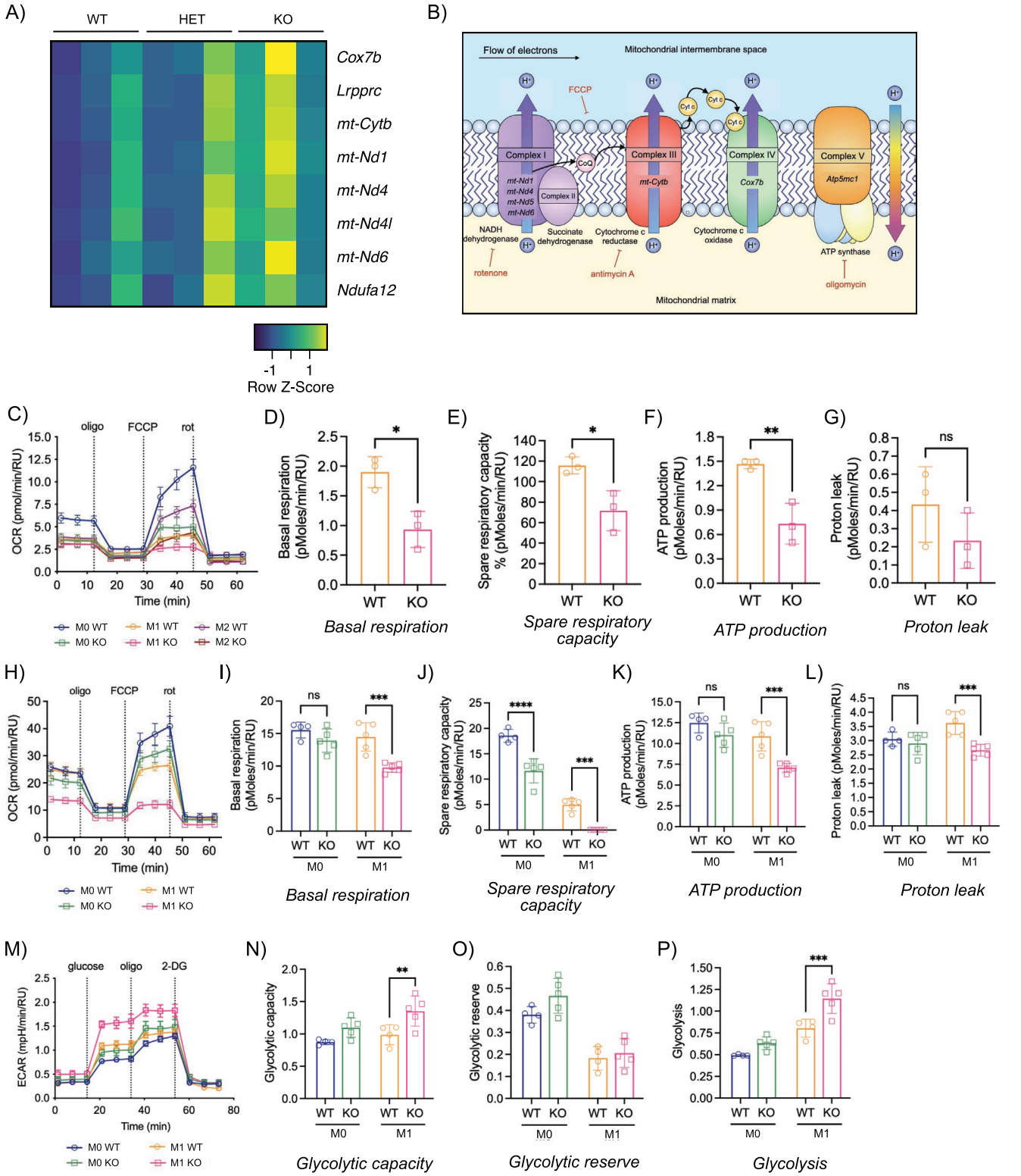

FIGURE 5 | Deficiency of PTPN2 in proinflammatory macrophages leads to metabolic reprogramming. (A–D) BMDMs were harvested from PTPN2 wild-type (WT), heterozygous (HET), and knockout (KO) mice and polarized toward M1 macrophages by stimulating them with IFN-ɣ and LPS for 24 h. (A) Heatmap of metabolic genes and specifically those relating to oxidative phosphorylation in M1 macrophages. (B) Diagram of electron transport chain and specific metabolic genes. (C–G) Seahorse XF assay performed with M0, M1, or M2 BMDMs derived from PTPN2 WT or KO mice to assess the oxygen consumption rate (OCR, C), basal respiration (D), spare respiratory capacity (SRC, E), ATP production (F), and proton leak (G). Data represent three biological replicate per genotype. *$p < 0.05$, **$p < 0.01$, based on *t*-test. (H–P) Seahorse XF assay performed with M0 and M1 BMDMs derived from PTPN2$^{fl/fl}$ LysM-Cre WT or KO mice to assess OCR (H) along with basal respiration (I), SRC (J), ATP production (K) and proton leak (L). The extracellular acidification rate (ECAR, M) was determined along with the glycolytic capacity (N), glycolytic reserve (O), and glycolysis (P). Data represents 4–5 mice per genotype. ***$p < 0.005$, ****$p < 0.0001$ based on two-way ANOVA with Šídák's multiple comparison test.

critical for tryptophan metabolism but also have immunosuppressive functions [56, 57]. We identified a similar upregulation of mitochondrially-encoded genes, which encode different subunits of Complex III (cytochrome B: *mt-Cytb*) and of Complex I (NADH dehydrogenase: *mt-Nd1*, *mt-Nd4*, *mt-Nd5*, and *mt-Nd6*) of the ETC (Figure S3D).

Knowing that several genes of the ETC were upregulated, we performed Seahorse XF analyses to assess the metabolic phenotype of these macrophages. We established that M1 macrophages perform mitochondrial respiration at a reduced rate compared to M0 and M2 macrophages and that this phenotype was even more pronounced in the absence of PTPN2 (Figure 5C). This also correlated with decreased basal respiration (Figure 5D), spare respiratory capacity (Figure 5E), ATP production (Figure 5F), and proton leak (Figure 5G) in proinflammatory PTPN2-deficient BMDMs, indicating that the absence of this phosphatase in M1 BMDMs specifically disrupts their capacity for respiratory metabolism and oxidative phosphorylation both in basal conditions and following a stress. We also identified the role of macrophage-specific PTPN2 deletion on mitochondrial respiration using BMDMs from PTPN2$^{fl/fl}$ LysM-Cre mice and performed similar Seahorse XF assays. Quantifying the oxygen consumption rate of these different macrophage populations (Figure 5H) allowed us to establish that depletion of PTPN2 in M1 BMDMs leads to a decrease in basal respiration (Figure 5I), spare respiratory capacity (Figure 5J), ATP production (Figure 5K), and proton leak (Figure 5L). Interestingly, PTPN2 deficiency in naive macrophages also results in reduced SRC, which is the maximal OCR that cells can undergo upon stress, in this case, characterized by the absence of PTPN2.

Considering the observed discrepancy between the transcriptional modulation of OXPHOS genes and the mitochondrial respiration in PTPN2-deficient M1 macrophages, we performed a different Seahorse XF assay, the glycolysis stress test, using PTPN2 LysM-Cre macrophages to study glycolysis specifically (Figure 5M). We found that while naïve macrophages were not unaffected by depletion of PTPN2, proinflammatory macrophages exhibited an increase in glycolytic capacity (Figure 5N) and glycolysis (Figure 5P). This increase in ECAR in the absence of PTPN2 is indicative of the Warburg effect.

4 | Discussion

Ablation of PTPN2 in mice leads to aberrant proinflammatory cytokine signaling that leads to systemic, overwhelming, and fatal inflammation [8]. We have also shown previously that this phosphatase negatively regulates macrophage development and differentiation [10, 11]. However, the role of PTPN2 in regulating the inflammatory phenotype and bioenergetics of macrophages has yet to be elucidated. In this study, we have demonstrated that PTPN2 dampens the proinflammatory immune response of macrophages. Systemic deletion of PTPN2 leads to upregulation of proinflammatory M1 markers at both the transcriptional and translational level, suggesting that PTPN2 deficiency skews macrophage polarization toward a proinflammatory subset. These have an altered transcriptome enriched in pathways involved with typical Th1 responses such as IFN-γ, PD-1, and TCR signaling, and antigen processing and presentation. We further demonstrated that these PTPN2-deficient proinflammatory macrophages have increased IFN-γ and nitric oxide production, which are crucial in promoting a Th1 immune response. Another interesting result we observed is the considerable downregulation of *Marco* in PTPN2-deficient M1 macrophages. MARCO-expressing TAMs have been shown to block the activation of cytotoxic T cells and NK cells, inhibiting their proliferation, cytokine production, and tumor-cell killing capacity [49]. In addition, antibodies against MARCO have been shown to slow growth and metastasis in syngeneic mouse tumor models by reprogramming M2-like TAMs into inflammatory M1-like macrophages. This switch involves reprogramming their metabolism [51, 58]. Similarly, targeting MARCO on human macrophages has been demonstrated to repolarize TAMs and to restore the cytotoxic, antitumor capacities of NK cells, and T cells [58, 59].

We demonstrated similar results in a myeloid-specific deletion of PTPN2 using a PTPN2/LysM-Cre mouse model that we generated. Another group has previously shown using this model that myeloid-specific deletion of PTPN2 in mice aggravated intestinal inflammation as induced by DSS, but protected them from colitis-associated tumor formation. They proposed that these inflammatory phenotypes resulted from upregulated IL-1β production caused by enhanced inflammasome activity [18]. However, they did not delve into macrophages' phenotype and associated functions. We demonstrated in PTPN2/LysM-Cre mice that PTPN2 inhibition enhances STAT1 and STAT3 hyperphosphorylation, likely inducing transcription of various proinflammatory and metabolic genes as we observed in our systemic mouse model.

Interestingly, STAT1 and STAT3 seem to be necessary for downstream ROS production [60–63]. Given that we observed an upregulation of metabolic pathways in our RNA-Seq M1 macrophage dataset, specifically those involved in mitochondrial respiration, the upregulation of STAT1 and STAT3 signaling pathways could favor NO and ROS production in PTPN2-deficient cells, eventually leading to aberrant use of mitochondria by these macrophages. We further showed that using a PTPN2 inhibitor on a human macrophage cell line leads to an increase in proinflammatory chemokines CXCL9, CXCL10, and CXCL11 at the transcriptional level, and of CXCL9 and CXCL10 at the protein level. These data solidify our previous discovery that PTPN2 depletion enhances the proinflammatory signature of macrophages.

Inhibition of PTPN2 in these cells affects not only their immune profile, but also their metabolic state. Pathway analysis and gene ontology enabled us to identify that respiratory electron transport and oxidative phosphorylation are enriched concomitantly with their enhanced proinflammatory state. However, we observed a decreased rate of mitochondrial respiration to almost undetectable levels in PTPN2-deficient proinflammatory macrophages, and this was accompanied by increased glycolysis and glycolytic capacity of these cells, typical of the Warburg effect [64].

Proinflammatory macrophages are known to undergo the Warburg effect and favor glycolysis, in which case their mitochondrial respiration would likely be considerably reduced

[7, 12]. Our data suggest that inhibiting PTPN2 could be sufficient in depleting Marco and reprogramming TAMs into tumor-suppressive M1 macrophages. Furthermore, a PTPN2 inhibitor could synergize with an anti-MARCO antibody to favor an antitumor response and be used as an immunotherapy treatment. More studies would be warranted to explore this question further.

Author Contributions

V.V. helped conceive the project, designed and performed the experiments, analyzed the data, and wrote and reviewed the manuscript. I.A. performed the western blots and Seahorse X.F. assays and analyzed the data. Y.Z. performed all bioinformatics analyses and figures. Z.M.C. performed experiments with the human macrophage cell line. M.L.T. helped conceive the project and wrote and reviewed the manuscript.

Acknowledgments

V.V. was a recipient of a Canderel Graduate Studentship award and a Seahorse Bioscience travel award. Y.Z. was a recipient of an FRQS scholarship. A.P. is a Canderel Studentship and FRQS doctoral scholarship recipient. ZCM was a recipient of an FRQS postdoctoral fellowship. M.L.T. Tremblay is a Distinguished James McGill Professor and the holder of the J and JL Levesque Chair in Cancer Research. This work was supported by the following funding agencies: Terry Fox oncometabolism grant TFF-116128, the Canadian Institute of Health Research Foundation grant (CIHR FDN-159923), the Richard and Edith Strauss Canada Foundation, and the Aclon Foundation. We thank Dr. Noriko Uetani for designing the graphical abstract.

Conflicts of Interest

The authors declare no conflicts of interest.

Data Availability Statement

The data that support the findings of this study are openly available in figshare at http://doi.org/10.6084/m9.figshare.27199401, reference number 10.6084/m9.figshare.27199401. Other data that support the findings of this study are available in the Section 3 and Supporting Information S1 sections of this article.

References

1. K. Murphy, P. Travers, and M. Walport, *Janeway's Immunobiology*, 7th ed. (Garland Publishing, 2008).

2. K. Murphy and C. Weaver, *Janeway's Immunobiology*, 9th ed. (Garland Science, 2017), https://doi.org/10.1201/9781315533247.

3. D. A. Chistiakov, V. A. Myasoedova, V. V. Revin, A. N. Orekhov, and Y. V. Bobryshev, "The Impact of Interferon-Regulatory Factors to Macrophage Differentiation and Polarization Into M1 and M2," *Immunobiology* 223 (2018): 101–111.

4. C. D. Mills, K. Kincaid, J. M. Alt, M. J. Heilman, and A. M. Hill, "M--1/M-2 Macrophages and the Th1/Th2 Paradigm," *Journal of Immunology* 164, no. 12 (2000): 6166–6173, https://doi.org/10.4049/jimmunol.164.12.6166.

5. A. J. Mouton, K. Y. DeLeon-Pennell, O. J. R. Gonzalez, et al., "Mapping Macrophage Polarization Over the Myocardial Infarction Time Continuum," *Basic Research in Cardiology* 113, no. 4 (2018): 26, https://doi.org/10.1007/s00395-018-0686-x.

6. M. Nahrendorf and F. K. Swirski, "Abandoning M1/M2 for a Network Model of Macrophage Function," *Circulation Research* 119 (2016): 414–417.

7. F. Wang, S. Zhang, R. Jeon, et al., "Interferon Gamma Induces Reversible Metabolic Reprogramming of M1 Macrophages to Sustain Cell Viability and pro-Inflammatory Activity," *eBioMedicine* 30 (2018): 303–316.

8. K. E. You-Ten, E. S. Muise, A. Itié, et al., "Impaired Bone Marrow Microenvironment and Immune Function in T Cell Protein Tyrosine Phosphatase–Deficient Mice," *Journal of Experimental Medicine* 186 (1997): 683–693.

9. K. M. Heinonen, "T-Cell Protein Tyrosine Phosphatase Deletion Results in Progressive Systemic Inflammatory Disease," *Blood* 103, no. 9 (2004): 3457–3464, https://doi.org/10.1182/blood-2003-09-3153.

10. P. D. Simoncic, A. Bourdeau, A. Lee-Loy, et al., "T-Cell Protein Tyrosine Phosphatase (Tcptp) is a Negative Regulator of Colony-Stimulating Factor 1 Signaling and Macrophage Differentiation," *Molecular and Cellular Biology* 26 (2006): 4149–4160.

11. K. M. Heinonen, A. Bourdeau, K. M. Doody, and M. L. Tremblay, "Protein Tyrosine Phosphatases PTP-1B and TC-PTP Play Nonredundant Roles in Macrophage Development and IFN-Gamma Signaling," *Proceedings. National Academy of Sciences. United States of America* 106, no. 23 (2009): 9368–9372, https://doi.org/10.1073/pnas.0812109106.

12. C. Li, Y. Wang, Y. Li, et al., "HIF1α-Dependent Glycolysis Promotes Macrophage Functional Activities in Protecting Against Bacterial and Fungal Infection," *Scientific Reports* 8 (2018): 3603, https://doi.org/10.1038/s41598-018-22039-9.

13. A. Viola, F. Munari, R. Sánchez-Rodriguez, S. Rommaso, and A. Castegna, "The Metabolic Signature of Macrophage Responses," *Frontiers in Immunology* 10, no. 1462 (2019): 1462, https://doi.org/10.3389/fimmu.2019.01462.

14. D. Qu, L. Shen, S. Liu, et al., "Chronic Inflammation Confers to the Metabolic Reprogramming Associated With Tumorigenesis of Colorectal Cancer," *Cancer Biology & Therapy* 18 (2017): 237–244.

15. V. Vinette, I. Aubry, H. Insull, N. Uetani, S. Hardy, and M. L. Tremblay, "Protein Tyrosine Phosphatome Metabolic Screen Identifies TC-PTP as a Positive Regulator of Cancer Cells Bioenergetics and Mitochondrial Dynamics," *FASEB Journal* 35, no. 7 (2021): e21708.

16. C. Penafuerte, L. A. Pérez-Quintero, V. Vinette, T. Hatzihristidis, and M. L. Tremblay, "Mining the Complex Family of Protein Tyrosine Phosphatases for Checkpoint Regulators in Immunity," in *Emerging Concepts Targeting Immune Checkpoints in Cancer and Autoimmunity*, vol. 410 (Springer, 2017), 499–524.

17. C. K. Baumgartner, H. Ebrahimi-Nik, A. Iracheta-Vellve, et al., "The PTPN2/PTPN1 Inhibitor ABBV-CLS-484 Unleashes Potent Anti-Tumour Immunity," *Nature* 622, no. 7984 (2023): 850–862, https://doi.org/10.1038/s41586-023-06575-7.

18. M. R. Spalinger, R. Manzini, L. Hering, et al., "PTPN2 Regulates Inflammasome Activation and Controls Onset of Intestinal Inflammation and Colon Cancer," *Cell Reports* 22 (2018): 1835–1848.

19. N. L. Bray, H. Pimentel, P. Melsted, and L. Pachter, "Near-Optimal Probabilistic RNA-Seq Quantification," *Nature Biotechnology* 34, no. 5 (2016): 525–527, https://doi.org/10.1038/nbt.3519.

20. C. Soneson, M. I. Love, and M. D. Robinson, "Differential Analyses for RNA-Seq: Transcript-Level Estimates Improve Gene-Level Inferences," *F1000Research* 4 (2015): 1521, https://doi.org/10.12688/f1000research.7563.2.

21. M. I. Love, W. Huber, and S. Anders, "Moderated Estimation of Fold Change and Dispersion for RNA-Seq Data With DESeq2," *Genome Biology* 15, no. 12 (2014): 550, https://doi.org/10.1186/s13059-014-0550-8.

22. A. Mantovani, A. Sica, S. Sozzani, P. Allavena, and A. Vecchi, "The Chemokine System in Diverse Forms of Macrophage Activation and Polarization," *Trends in Immunology* 25, no. 12 (2004): 677–686, https://doi.org/10.1016/j.it.2004.09.015.

23. F. O. Martinez, S. Gordon, M. Locati, and A. Mantovani, "Transcriptional Profiling of the Human Monocyte-To-Macrophage Differentiation

and Polarization: New Molecules and Patterns of Gene Expression," *Journal of Immunology* 177, no. 10 (2006): 7303–7311, https://doi.org/10.4049/jimmunol.177.10.7303.

24. F. O. Martinez, A. Sica, A. Mantovani, and M. Locati, "Macrophage Activation and Polarization," *Frontiers in Bioscience* 13 (2008): 453–461.

25. W. Ying, P. S. Cheruku, F. W. Bazer, S. H. Safe, and B. Zhou, "Investigation of Macrophage Polarization Using Bone Marrow Derived Macrophages," *Journal of Visualized Experiments* 23, no. 76 (2013): 50323, https://doi.org/10.3791/50323.

26. L. S. Bisgaard, C. K. Mogensen, A. Rosendahl, et al., "Bone Marrow-Derived and Peritoneal Macrophages Have Different Inflammatory Response to oxLDL and M1/M2 Marker Expression - Implications for Atherosclerosis Research," *Scientific Reports* 6 (2016): 35234, https://doi.org/10.1038/srep35234.

27. S. Oishi, R. Takano, S. Tamura, et al., "M2 Polarization of Murine Peritoneal Macrophages Induces Regulatory Cytokine Production and Suppresses T-Cell Proliferation," *Immunology* 149 (2016): 320–328.

28. Y. L. Zhao, P. X. Tian, F. Han, et al., "Comparison of the Characteristics of Macrophages Derived From Murine Spleen, Peritoneal Cavity, and Bone Marrow," *Journal of Zhejiang University. Science. B* 18, no. 12 (2017): 1055–1063, https://doi.org/10.1631/jzus.B1700003.

29. T. Yu, S. Gan, Q. Zhu, et al., "Modulation of M2 Macrophage Polarization by the Crosstalk Between Stat6 and Trim24," *Nature Communications* 10, no. 1 (2019): 4353, https://doi.org/10.1038/s41467-019-12384-2.

30. B. Pourcet and I. Pineda-Torra, "Transcriptional Regulation of Macrophage Arginase 1 Expression and Its Role in Atherosclerosis," *Trends in Cardiovascular Medicine* 23 (2013): 143–152, https://doi.org/10.1016/j.tcm.2012.10.003.

31. X. Lu, J. Chen, R. T. Sasmono, et al., "T-Cell Protein Tyrosine Phosphatase, Distinctively Expressed in Activated-B-Cell-Like Diffuse Large B-Cell Lymphomas, Is the Nuclear Phosphatase of STAT6," *Molecular and Cellular Biology* 27 (2007): 2166–2179.

32. H. Namkoong, M. Y. Song, Y. B. Seo, et al., "Enhancement of Antigen-Specific CD8 T Cell Responses by Co-Delivery of Fc-Fused CXCL11," *Vaccine* 32, no. 10 (2014): 1205–1212, https://doi.org/10.1016/j.vaccine.2013.07.066.

33. P. Meiser, M. A. Knolle, A. Hirschberger, et al., "A Distinct Stimulatory cDC1 Subpopulation Amplifies $CD8^+$ T Cell Responses in Tumors for Protective Anti-Cancer Immunity," *Cancer Cell* 41, no. 8 (2023): 1498–1515, https://doi.org/10.1016/j.ccell.2023.06.008.

34. G. Schreibelt, L. J. Klinkenberg, L. J. Cruz, et al., "The C-Type Lectin Receptor CLEC9A Mediates Antigen Uptake and (Cross-)presentation by Human Blood BDCA3+ Myeloid Dendritic Cells," *Blood* 119, no. 10 (2012): 2284–2292, https://doi.org/10.1182/blood-2011-08-373944.

35. C. M. Henry, C. A. Castellanos, M. D. Buck, et al., "SYK Ubiquitination by CBL E3 Ligases Restrains Cross-Presentation of Dead Cell-Associated Antigens by Type 1 Dendritic Cells," *Cell Reports* 42, no. 12 (2023): 113506, https://doi.org/10.1016/j.celrep.2023.113506.

36. J. G. Zhang, P. E. Czabotar, A. N. Policheni, et al., "The Dendritic Cell Receptor Clec9A Binds Damaged Cells via Exposed Actin Filaments," *Immunity* 36, no. 4 (2012): 646–657, https://doi.org/10.1016/j.immuni.2012.03.009.

37. A. Salminen, "Role of Indoleamine 2,3-Dioxygenase 1 (IDO1) and Kynurenine Pathway in the Regulation of the Aging Process," *Ageing Research Reviews* 75 (2022): 101573, https://doi.org/10.1016/j.arr.2022.101573.

38. G. Guo, L. Sun, L. Yang, and H. Xu, "IDO1 Depletion Induces an Anti-Inflammatory Response in Macrophages in Mice With Chronic Viral Myocarditis," *Cell Cycle* 18, no. 20 (2019): 2598–2613, https://doi.org/10.1080/15384101.2019.1652471.

39. T. Kawasaki and T. Kawai, "Toll-Like Receptor Signaling Pathways," *Frontiers in Immunology* 5 (2014): 461, https://doi.org/10.3389/fimmu.2014.00461.

40. T. Kawai and S. Akira, "The Role of Pattern-Recognition Receptors in Innate Immunity: Update on Toll-Like Receptors," *Nature Immunology* 11, no. 5 (2010): 373–384, https://doi.org/10.1038/ni.1863.

41. T. J. Vanden Bush and G. A. Bishop, "TLR7 and CD40 Cooperate in IL-6 Production via Enhanced JNK and AP-1 Activation," *European Journal of Immunology* 38, no. 2 (2008): 400–409, https://doi.org/10.1002/eji.200737602.

42. S. Chaudhari, B. M. D'Souza, J. Y. Morales, et al., "Renal TLR-7/TNF-α Pathway as a Potential Female-Specific Mechanism in the Pathogenesis of Autoimmune-Induced Hypertension," *American Journal of Physiology. Heart and Circulatory Physiology* 323, no. 6 (2022): H1331–H1342, https://doi.org/10.1152/ajpheart.00286.2022.

43. J. Lee, Y. Tian, S. T. Chan, J. Y. Kim, C. Cho, and J. H. Ou, "TNF-α Induced by Hepatitis C Virus via TLR7 and TLR8 in Hepatocytes Supports Interferon Signaling via an Autocrine Mechanism," *PLoS Pathogens* 11, no. 5 (2015): e1004937, https://doi.org/10.1371/journal.ppat.1004937.

44. M. Archer, S. M. Bernhardt, L. J. Hodson, et al., "CCL2-Mediated Stromal Interactions Drive Macrophage Polarization to Increase Breast Tumorigenesis," *International Journal of Molecular Sciences* 24, no. 8 (2023): 7385, https://doi.org/10.3390/ijms24087385.

45. M. Keophiphath, C. Rouault, A. Divoux, K. Clément, and D. Lacasa, "CCL5 Promotes Macrophage Recruitment and Survival in Human Adipose Tissue," *Arteriosclerosis, Thrombosis, and Vascular Biology* 30, no. 1 (2010): 39–45, https://doi.org/10.1161/ATVBAHA.109.197442.

46. T. Yoshimura, E. A. Robinson, S. Tanaka, E. Appella, and E. J. Leonard, "Purification and Amino Acid Analysis of Two Human Monocyte Chemoattractants Produced by Phytohemagglutinin-Stimulated Human Blood Mononuclear Leukocytes," *Journal of Immunology* 142 (1989): 1956–1962.

47. T. Yoshimura, N. Yuhki, S. K. Moore, E. Appella, M. I. Lerman, and E. J. Leonard, "Human Monocyte Chemoattractant Protein-1 (MCP-1). Full-Length cDNA Cloning, Expression in Mitogen- Stimulated Blood Mononuclear Leukocytes, and Sequence Similarity to Mouse Competence Gene JE," *FEBS Letters* 244 (1989): 487–493.

48. S. L. Deshmane, S. Kremlev, S. Amini, and E. S. Sawaya, "Monocyte Chemoattractant Protein-1 (MCP-1): An Overview," *Journal of Interferon & Cytokine Research* 29, no. 6 (2009): 313–326, https://doi.org/10.1089/jir.2008.0027.

49. J. Jing, I. V. Yang, L. Hui, et al., "Role of MARCO in Innate Immune Tolerance," *Journal of Immunology* 190, no. 12 (2013): 6360–6367.

50. K. E. Novakowski, A. Huynh, S. Han, et al., "A Naturally Occurring Transcript Variant of MARCO Reveals the SRCR Domain Is Criticial for Function," *Immunology and Cell Biology* 94, no. 7 (2016): 646–655.

51. A. M. Georgoudaki, K. E. Prokopec, V. F. Boura, et al., "Reprogramming Tumor-Associated Macrophages by Antibody Targeting Inhibits Cancer Progression and Metastasis," *Cell Reports* 15, no. 9 (2016): 2000–2011, https://doi.org/10.1016/j.celrep.2016.04.084.

52. A. E. Boniakowski, A. S. Kimball, A. Joshi, et al., "Murine Macrophage Chemokine Receptor CCR2 Plays a Crucial Role in Macrophage Recruitment and Regulated Inflammation in Wound Healing," *European Journal of Immunology* 48, no. 9 (2018): 1445–1455.

53. B. E. Clausen, C. Burkhardt, W. Reith, R. Renkawitz, and I. Förster, "Conditional Gene Targeting in Macrophages and Granulocytes Using LysMcre Mice," *Transgenic Research* 8, no. 4 (1999): 265–277, https://doi.org/10.1023/a:1008942828960.

54. K. Takeda, B. E. Clausen, T. Kaisho, et al., "Enhanced Th1 Activity and Development of Chronic Enterocolitis in Mice Devoid of Stat3 in Macrophages and Neutrophils," *Immunity* 10 (1999): 39–49.

55. S. Le Sommer, N. Morrice, M. Pesaresi, et al., "Deficiency in Protein Tyrosine Phosphatase PTP1B Shortens Lifespan and Leads to Development of Acute Leukemia," *Cancer Research* 78 (2018): 75–87.

56. M. Liu, X. Wang, L. Wang, et al., "Targeting the IDO1 Pathway in Cancer: From Bench to Bedside," *Journal of Hematology & Oncology* 11, no. 1 (2018): 100, https://doi.org/10.1186/s13045-018-0644-y.

57. G. C. Prendergast, C. Smith, S. Thomas, et al., "Indoleamine 2,3-Dioxygenase Pathways of Pathogenic Inflammation and Immune Escape in Cancer," *Cancer Immunology, Immunotherapy* 63, no. 7 (2014): 721–735, https://doi.org/10.1007/s00262-014-1549-4.

58. S. Eisinger, D. Sarhan, V. F. Boura, et al., "Targeting a Scavenger Receptor on Tumor-Associated Macrophages Activates Tumor Cell Killing by Natural Killer Cells," *Proceedings of the National Academy of Sciences of the United States of America* 117, no. 50 (2020): 32005–32016, https://doi.org/10.1073/pnas.2015343117.

59. L. La Fleur, J. Botling, F. He, et al., "Targeting MARCO and IL37R on Immunosuppressive Macrophages in Lung Cancer Blocks Regulatory T Cells and Supports Cytotoxic Lymphocyte Function," *Cancer Research* 81, no. 4 (2021): 956–967, https://doi.org/10.1158/0008-5472.CAN-20-1885.

60. J. A. Meier, M. Hyun, M. Cantwell, et al., "Stress-Induced Dynamic Regulation of Mitochondrial STAT3 and Its Association With Cyclophilin D Reduce Mitochondrial ROS Production," *Science Signaling* 10, no. 472 (2017): eaag2588.

61. J. D. Sisler, M. Morgan, V. Raje, et al., "The Signal Transducer and Activator of Transcription 1 (STAT1) Inhibits Mitochondrial Biogenesis in Liver and Fatty Acid Oxidation in Adipocytes," *PLoS One* 10, no. 12 (2015): e0144444.

62. A. H. Kramer, R. Kadye, P. S. Houseman, and E. Prinsloo, "Mitochondrial STAT3 and Reactive Oxygen Species: A Fulcrum of Adipogenesis?," *JAK-Stat* 4 (2015): 1–10.

63. J. A. Meier and A. C. Larner, "Toward a New STATe: The Role of STATs in Mitochondrial Function," *Seminars in Immunology* 26, no. 1 (2014): 20–28, https://doi.org/10.1016/j.smim.2013.12.005.

64. M. D. Kornberg, "The Immunologic Warburg Effect: Evidence and Therapeutic Opportunities in Autoimmunity," *Wiley Interdisciplinary Reviews. Systems Biology and Medicine* 12, no. 5 (2020): e1486, https://doi.org/10.1002/wsbm.1486.

Supporting Information

Additional supporting information can be found online in the Supporting Information section.